

Homoclinic Bifurcations for Partial Differential Equations in Unbounded Domains

By A. C. Fowler

The connection between low-dimensional chaos in ordinary differential equations, and turbulence in fluids and other systems governed by partial differential equations, is one that is in many circumstances not clear. We discuss some examples of turbulent fluid flow, and consider ways in which they may be related to much simpler sets of ordinary differential equations, whose behavior can be reasonably well understood. (We are *not* advocating drastic Fourier truncation.) The generation of aperiodic solutions through the occurrence of homoclinic orbits is briefly analysed for ordinary differential equations, and the same kind of heuristic analysis is sketched for partial differential equations (in one space dimension). It is suggested that such an analysis can explain certain features of chaos, which have been observed in real fluids.

1. Introduction

The rapid development of the study of chaos in the last twenty-five years has been partly fueled by the wide variety of its applications, in such diverse fields as meteorology, population biology, reaction chemistry, Hamiltonian dynamics, and fluid dynamics. Eckmann [6] identified several "routes" towards chaos, and these have proved useful in understanding observations in certain fluid-dynamical experiments, notably in the Taylor-Couette experiment [7] and in thermal convection (Libchaber et al. [16]). But in other, more long-standing problems, for example the transition to turbulence in shear flows, there are no such obvious analogous phenomena, and the relationship between chaos and turbulence is less clear.

Address for correspondence: Dr. A. C. Fowler, Mathematical Institute, Oxford University, 24-29 St. Giles', Oxford OX1 3LB, England.

In this context, I would like to quote Ed Spiegel [25]: "ordinary chaos is not turbulence, but turbulence is chaotic." In a sense, this virtually follows from a definition of chaos as being long-term aperiodic behavior of a deterministic system. Two questions (amongst others) naturally arise: firstly, can we understand how chaos arises in ordinary differential equations, and if so, can we extend this knowledge to partial differential equations, *in a predictive way*?

The idea of describing different routes to chaos is not quite what we want here, because in experimental systems, these are really diagnostic rather than predictive tools. We understand period doubling in (for example) convection, because we know it happens in one-dimensional maps, but we cannot then predict what the resulting chaos "looks" like. Secondary and tertiary Hopf bifurcation (the Ruelle-Takens scenario) has the same problem. One may suppose that the Taylor-Couette transition (one frequency, two frequencies, low-amplitude noise) corresponds to the final appearance of a third frequency—but one does not know: the diagnostic tool breaks down when the chaos is reached.

Part of the problem with such diagnostic routes is that they say nothing about the flow trajectories themselves. When their hallmarks are absent (as in shear flow), there is no real substitute. What I wish to do in this paper is to describe how homoclinic bifurcation analysis, as developed for ordinary differential equations [20–22], can be extended (at least in a formal manner) to partial differential equations. Homoclinic bifurcations can "produce" a strange invariant set (i.e., an invariant set which contains countably many periodic orbits and uncountably many aperiodic orbits), in the same sense that a Hopf bifurcation "produces" a periodic orbit. Thus we can reasonably expect to observe chaotic behavior when a finite-dimensional system possesses one or more homoclinic orbits. Occurrence of homoclinic orbits is a codimension-one phenomenon, which implies that chaotic solutions may "generally" occur as one varies a single parameter.

Finite-dimensional chaos might be expected to resemble, in a crude way, the trajectory structure which is observed near the homoclinic bifurcation. In a similar vein, we may hope that the structure of the invariant set, produced near a homoclinic bifurcation in a partial differential equation, may bear some resemblance to some features which are observed in numerical and laboratory experiments.

In what follows, we shall firstly describe some features of shear flow turbulence and thermal convection which suggest that homoclinic bifurcations may have some relevance to these situations. In Sections 2 and 3, we summarize the approximate derivation of a Poincaré map for o.d.e.'s and p.d.e.'s, respectively, and show how it can be reduced to a first- or second-order difference equation. Finally, we hazard some interpretations of these results, and end with some speculation on their relevance to fluid experiments.

Shil'nikov and Lorenz

The fundamental ideas of homoclinic bifurcation go back to Poincaré, but for dissipative systems were principally expounded by Shil'nikov [20–22] on the

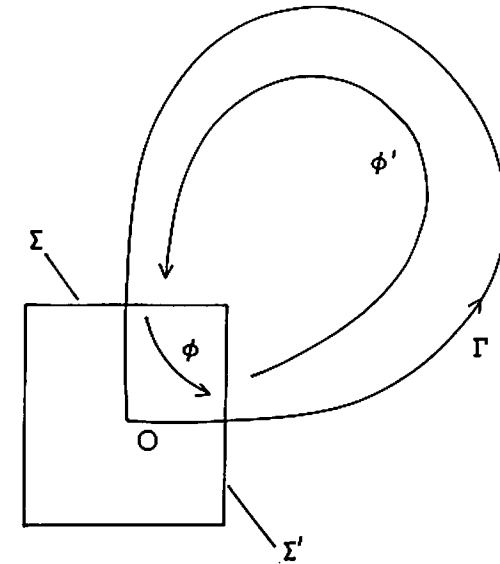


Figure 1. Schematic representation of the procedure for constructing a Poincaré map. Orbits near the homoclinic orbit Γ pass successively through Σ and Σ' . The map ϕ from Σ to Σ' represents the approximately linear flow, while the map ϕ' from Σ' to Σ is approximately affine.

assumption that there is oscillatory behavior near the origin (which is taken to be a fixed point of the system). His methods were taken up by Tresser (e.g. [28]) and Arneodo et al. [2], and applied by Sparrow [23] to the Lorenz [17] equations, in which there is a natural symmetry. The basic idea is that, if a system of ordinary differential equations $\dot{x} = f(x, \mu)$ possesses a homoclinic orbit Γ (i.e., one which is asymptotic to a fixed point $x = 0$ as $t \rightarrow \pm\infty$) when the parameter $\mu = 0$, then for small values of μ , and for x initially close to Γ , there may be recurrent trajectories which remain close to Γ for all t . Generally, this *invariant set* may consist of a single periodic orbit, or may be *strange*, that is, it may contain countably many periodic orbits and uncountably many aperiodic orbits. All such orbits are typically unstable, as is the invariant set, but other bifurcations can render the invariant set attracting, so that we obtain a "strange attractor," as for instance in the Lorenz equations. Thus the occurrence of chaotic behavior in ordinary differential equations may often be associated with homoclinic bifurcation. Furthermore, these bifurcations typically "produce" period-doubling sequences, so that this latter route to chaos may simply be viewed as a consequence of the homoclinic bifurcation.

The basis for the analysis is shown in Figure 1. We take Σ and Σ' as faces of a box at the origin, respectively transverse to the stable manifold W_s and the

unstable manifold W_U . If the box is small, then we approximate the flow within by linearizing about 0. This gives a map φ from Σ to Σ' . From Σ' to Σ , the trajectory is close to Γ , so the system may be linearized about Γ , and one finds that the map φ' from Σ' to Σ is approximately affine. The composition of φ and φ' defines a Poincaré map Φ from Σ to Σ . Even in n dimensions, this map [which is then $(n-1)$ -dimensional] is close to a one-dimensional map. Periodic orbits of the flow correspond to fixed points of the one-dimensional map by a use of the implicit-function theorem. Aperiodic orbits exist close to the periodic orbits, because one can show that there are horseshoes embedded in the Poincaré map [8].

What can any of this possibly have to do with turbulence in fluids? There are two situations we shall mention. Transition to turbulence in shear flows has generated an enormous literature since Reynolds's pioneering experiments one hundred years ago. Much of this literature has been concerned with linear instability, and later, nonlinear instability [26, 18]. Although much of this analysis can be quite sophisticated, it is conceptually based on the idea that transition is associated with what is essentially a Hopf bifurcation, and thus is fundamentally unable to describe directly the irregular behavior which is observed. The field of nonlinear stability studies has been very fruitful, and has provided a platform for more recent semi-numerical work [12, 19], which goes some way towards elucidating the mechanism of transition. Despite this, the issue of how irregular trajectories in the governing equations come into existence has not been addressed.

It is very tempting to draw an analogy between the Lorenz equations, which numerically exhibit an abrupt jump to chaos when the bifurcation parameter r increases beyond a critical value where a subcritical Hopf bifurcation occurs, and transition in plane Poiseuille flow, which exhibits an abrupt transition to turbulent motion when the Reynolds number Re increases beyond about 1000, whereas there is a subcritical Hopf bifurcation at $Re \approx 5772$. It is an obvious speculation that transition to turbulence in shear flow is caused by the existence of a homoclinic orbit, and that the bifurcation associated with such an orbit is what causes the irregular flow. It is in the direction of this idea that the present paper is aimed.

There is perhaps more evidence that thermal "turbulence" (i.e. at large Rayleigh number, but not large Reynolds number) is associated with homoclinic structure. Apart from the known existence of homoclinic orbits in Fourier truncations of the convection equations (e.g. the Lorenz equations), experimental observations suggest that thermal turbulence often takes the form of sporadic eruption of "thermals" from the boundary layers, which rise or fall through the fluid to the other boundary [24, 27, 13]. These features bear all the hallmarks of homoclinic orbits.

From the above remarks, it will be evident that the present research has as its long-term goal the adaption of numerical orbit-following programs to partial differential equations, with a view to locating homoclinic orbits for the Navier-Stokes equations. In this way it is hoped that some fundamental understanding may arise as to just what turbulent motion might consist of. This paper takes a step in that direction. In the next section, we show how to do the bifurcation

analysis for a system of ordinary differential equations; this summarizes work presented recently by Fowler [8]. We restate it here, as it is a necessary prerequisite to understanding the formalism, which is then applied to a certain class of partial differential equations in the subsequent section, namely evolution equations in one space dimension on an infinite domain.

2. Homoclinic bifurcations for ordinary differential equations

Consider the system of ordinary differential equations

$$\dot{x} = f(x, \mu), \quad (2.1)$$

where $x \in \mathbb{R}^n$, $\mu \in \mathbb{R}$, and f is smooth (e.g. analytic). Suppose

$$f(0, \mu) = 0, \quad (2.2)$$

and that when $\mu = 0$, there exists a homoclinic orbit to the origin:

$$\Gamma: x = x^*(t), \quad x^* \rightarrow 0 \quad \text{as } t \rightarrow \pm\infty. \quad (2.3)$$

We can assume that the coordinate basis for x is such that $Df(0; \mu)$ is diagonal (this may require complexification of the components of x), and that the stable and unstable manifolds W_S and W_U at the origin are locally identical to the tangent eigenspaces. Generally, we let suffixes U and S denote components in W_U and W_S , so that, for example, $x = (x_U, x_S)$, etc. We define

$$D(\mu) = Df(0; \mu); \quad (2.4)$$

then there are vectors $\alpha^* = (\alpha_U^*, 0)^T$, $\beta^* = (0, \beta_S^*)^T$ satisfying $x^* \sim \exp(tD_0)\alpha^*$ as $t \rightarrow -\infty$, $x^* \sim \exp(tD_0)\beta^*$ as $t \rightarrow +\infty$, and we may choose the phase of x^* such that α^* , $\beta^* = O(1)$. We define α^* and β^* more precisely as follows: define the return surfaces Σ and Σ' by

$$\begin{aligned} \Sigma: | \langle x, e^S \rangle | &= \nu, \\ \Sigma': | \langle x, e^U \rangle | &= \nu K, \quad K = O(1), \end{aligned} \quad (2.5)$$

where $\nu \ll 1$, and e^S and e^U are the eigenvectors in W_S and W_U whose corresponding eigenvalues have their real parts closest to zero. The precise value of K is a technical detail. Thus $x^*(t)$ intersects Σ when $t = t_S \gg 1$, and intersects Σ' when $t = -t_U$, $t_U \gg 1$. With these definitions of t_U and t_S , we define α , β , α^* , β^* , $\tilde{\alpha}$, and $\tilde{\beta}$ by

$$\begin{aligned} x^* &= \exp(-t_U D_0) \alpha^* \quad \text{on } \Sigma', \quad | \langle \alpha^*, e^U \rangle | = 1, \\ x^* &= \exp(t_S D_0) \beta^* \quad \text{on } \Sigma, \quad | \langle \beta^*, e^S \rangle | = 1, \end{aligned} \quad (2.6)$$

and more generally

$$\begin{aligned}x &= \exp(-t_U D_0) \alpha \quad \text{on } \Sigma', \\x &= \exp(t_S D_0) \beta \quad \text{on } \Sigma.\end{aligned}\quad (2.7)$$

Within the box B , we have

$$\begin{aligned}\dot{x} &= Dx + g(x), \\g(x) &= f(x, \mu) - Df(0; \mu)x = O(x^2),\end{aligned}\quad (2.8)$$

or equivalently, if $x = x_0$ at $t = t_0$,

$$x = \exp[(t - t_0)D] x_0 + \int_{t_0}^t \exp[(t - t_0 - \tau)D] g[x(\tau)] d\tau. \quad (2.9)$$

Using (2.7), and letting \tilde{t} be the time of transit from Σ to Σ' , we find that (2.9) is approximately given by

$$\alpha = e^{PD} \beta, \quad (2.10)$$

[8], where P is the return time between passages of x through Σ , and is given by

$$P = t_U + t_S + \tilde{t}. \quad (2.11)$$

Notice that orbits close to x^* in Σ and Σ' correspond to values of α and β of $O(1)$.

To map the flow from Σ' back to Σ , we write

$$x(t) = x^*(t) + y(t), \quad (2.12)$$

so that y satisfies

$$\dot{y} = A_\Gamma(t)y + \mu \frac{\partial f}{\partial \mu}(x^*, 0) + G(t; y), \quad (2.13)$$

where

$$A_\Gamma = Df(x^*(t), \mu),$$

$$G = f(x^* + y, 0) - f(x^*, 0) - Df(x^*, 0)y - \mu \frac{\partial f}{\partial \mu}(x^*, 0). \quad (2.14)$$

We define $\Psi(t)$ to be a fundamental matrix for the linear system

$$\dot{y} = A_\Gamma y, \quad (2.15)$$

and then define H by

$$\Psi = \exp(tD_0) H(t). \quad (2.16)$$

We can assume that

$$H(-\infty) = I, \quad H(\infty) = M \quad (\text{constant}). \quad (2.17)$$

The solution of (2.13) with initial data $y = y_0$ at $t = t_0$ is

$$y = \Psi(t)^{-1} \Psi(t_0) y_0 + \Psi(t) \int_{t_0}^t \Psi^{-1}(s) \left[G[s; y(s)] + \mu \frac{\partial f}{\partial \mu}(x^*, 0) \right] ds. \quad (2.18)$$

Using (2.6) and (2.7), we find (approximately)

$$\beta' - \beta^* = M(\alpha - \alpha^*) + \mu c, \quad (2.19)$$

where β' is the value of β on Σ at the next passage of the orbit through Σ .

We have shown here how an approximate Poincaré map can be derived for systems near a homoclinic bifurcation. Wiggins [30] has shown that, if this approximation is smooth, then results for the approximate map carry over to the actual map. Without further ado, we therefore confine ourselves to a consideration of the approximate Poincaré map from Σ to Σ which takes β to β' :

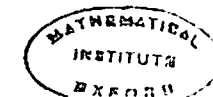
$$\alpha = e^{PD} \beta, \quad (2.20)$$

$$\beta' - \beta^* = M(\alpha - \alpha^*) + \mu c.$$

A one-dimensional map

Now P is the return time between intersections with Σ , and if α, β are close to α^*, β^* , then P will be large. Specifically, if $\beta - \beta^* \leq \delta \ll 1$, where $\delta \geq \mu$, then we require $\alpha - \alpha^* \leq \delta$ also. It is convenient to choose coordinates $a_U \in W_U, b_S \in W_S$ defined by

$$\alpha_U = \alpha_U^* + a_U, \quad \beta_S = \beta_S^* + b_S; \quad (2.21)$$



thus $a_U, b_S \leq \delta$, and we project the map (2.20) onto W_S and W_U as

$$\begin{aligned}\beta_U &= e^{-PD_U}(\alpha_U^* + a_U), \\ \alpha_S &= e^{PD_S}(\beta_S^* + b_S), \\ b_S' &= M_{SU}a_U + M_{SS}\alpha_S + \mu c_S, \\ \beta_U' &= M_{UU}a_U + M_{US}\alpha_S + \mu c_U,\end{aligned}\quad (2.22)$$

where we have defined

$$M = \begin{pmatrix} M_{UU} & M_{US} \\ M_{SU} & M_{SS} \end{pmatrix}, \quad (2.23)$$

and $D_U = D|_{W_U}$, $D_S = D|_{W_S}$. Evidently, we need to restrict attention in Σ (and Σ') to neighborhoods of the sets

$$\begin{aligned}\Lambda_0 \subset \Sigma: \beta_U &= e^{-PD_U}\alpha_U^*, \\ \Lambda_0 \subset \Sigma': \alpha_S &= e^{PD_S}\beta_S^*,\end{aligned}\quad (2.24)$$

as points away from these sets will not be mapped back to Σ . Also evidently, $\Lambda_0 \cap W_U$ is a one-dimensional set parameterized by P ; thus, since we are only concerned with points which continue to be mapped to Σ , we restrict our interest to points $\beta' \in \Sigma$ which are close to Λ_0 :

$$\beta_U' = e^{-PD_U}(\alpha_U^* + a_U'). \quad (2.25)$$

Evidently, we can use (2.22)₁ to define P and a_U in terms of β_U , since we can, for example, always choose

$$\langle a_U, e^U \rangle = 0. \quad (2.26)$$

Thus, if W_U is k -dimensional, so is β_U , a_U is $(k-1)$ -dimensional, and P is one-dimensional. Hence, we choose to map the $(n-1)$ -dimensional triple (a_U, b_S, P) to the succeeding values (a_U', b_S', P') . Since W_S is $(n-k)$ -dimensional, and (2.5)₁ implies

$$\langle b_S, e^S \rangle = 0, \quad (2.27)$$

then b_S is $(n-k-1)$ -dimensional. Rewriting (2.22) with (2.25), we have

$$\begin{aligned}b_S' &= M_{SU}a_U + M_{SS}e^{PD_S}(\beta_S^* + b_S) + \mu c_S, \\ e^{-PD_U}(\alpha_U^* + a_U') &= M_{UU}a_U + M_{US}e^{PD_S}(\beta_S^* + b_S) + \mu c_U.\end{aligned}\quad (2.28)$$

Since the eigenvalues of D_S have negative real part, and those of D_U have positive real part, we see that $|e^{PD_S}|, |e^{-PD_U}| \ll 1$ (and in fact, $\leq \delta$). It is then evident from (2.28) that

$$\begin{aligned}b_S' &\approx M_{SU}a_U + M_{SS}e^{PD_S}\beta_S^* + \mu c_S, \\ M_{UU}a_U &\approx e^{-PD_U}\alpha_U^* - M_{US}e^{PD_S}\beta_S^* - \mu c_U.\end{aligned}\quad (2.29)$$

If we define the spaces spanned by a_U and b_S as Σ_U and Σ_S , with P parametrizing Λ_0 , then the implication of (2.29) is that under the Poincaré map, Σ_U is uniformly expanded, whereas Σ_S is uniformly contracted, so that we have the basic ingredients of a hyperbolic structure. Furthermore, although a_U is $(k-1)$ -dimensional and M_{UU} is a $k \times k$ matrix, (2.29)₂ is not inconsistent, since one can show that, when $\mu = 0$, the rank of M_{UU} is $k-1$ (since $M_{UU}D_U\alpha_U^* = 0$). If η is the unique eigenvector of the Hermitian adjoint of M_{UU} (at $\mu = 0$), then we can determine P' explicitly via the (approximate) one-dimensional map

$$\langle \eta, e^{-PD_U}\alpha_U^* \rangle = \langle \eta, M_{US}e^{PD_S}\beta_S^* \rangle + \mu \langle \eta, c_U \rangle. \quad (2.30)$$

One has to be rather careful as to how one interprets (2.30). Fixed points of (2.30) imply, by using the implicit-function theorem, the existence of corresponding fixed points of (2.28), and hence periodic orbits for the flow. Aperiodic trajectories of (2.30) may not necessarily correspond to aperiodic orbits of the flow. However, if σ^U and σ^S are the eigenvalues of D_U and D_S with real part closest to zero (i.e. correspond to e^U and e^S), then if σ^U is complex and $\text{Re } \sigma^U < |\text{Re } \sigma^S|$, one can show that there are horseshoes embedded in the flow. Figure 2 depicts the general idea (cf. [30]). Provided one interprets it appropriately, one can thus use (2.30) as a descriptor of the dynamics of the flow.

As an example, we consider the Shil'nikov case, $\sigma^U = \lambda^U \pm i\omega^U$, $\sigma^S = -\lambda^S$, $\lambda^U < \lambda^S$, with other eigenvalues having real parts further from zero. (2.30) can then be approximated by

$$e^{-\lambda^U P'} \cos(\omega^U P') = a e^{-\lambda^S P} + \mu, \quad (2.31)$$

where we have rescaled P as necessary. With $\lambda^S > \lambda^U$, fixed points satisfy

$$\mu \sim e^{-\lambda^U P} \cos(\omega^U P) \quad (2.32)$$

as $P \rightarrow \infty$, giving the well-known multiplicity of periodic orbits as $\mu \rightarrow 0$ [10,9]. There also exist uncountably many aperiodic orbits which are homeomorphic to a shift on N symbols, where N tends to infinity as $\mu \rightarrow 0$.

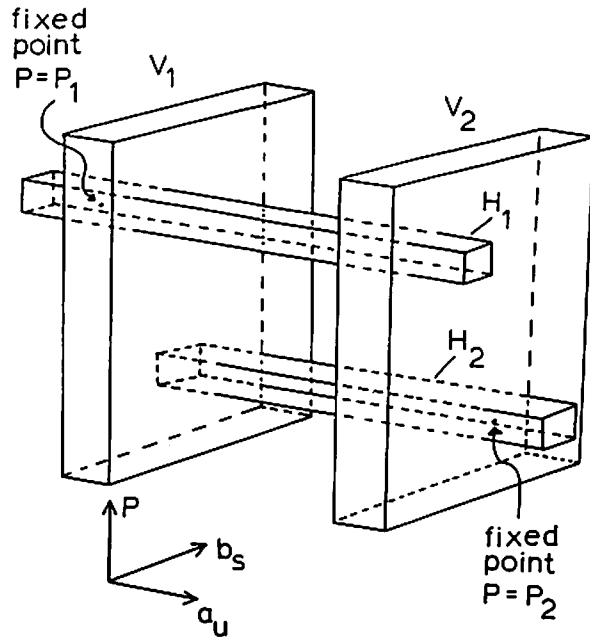


Figure 2. If we suppose that the one-dimensional map is multivalued and has (at least) two fixed points with $P = P_1$, $P = P_2$, then the sets V_1 and V_2 containing these fixed points are mapped under the flow to sets H_1 and H_2 which are much fatter in W_U , much thinner in W_S . If, in addition, the map is strongly contractive of an interval of P values (it need not be uniformly contractive), then the sets $H_i \cap V_j$ are nonempty. Further iteration of the map then generates a strange invariant set inside

3. Homoclinic bifurcations for partial differential equations

In this section, we repeat the formalism of the finite-dimensional case. While there are serious technical issues which still need to be addressed, the practical method of calculation should be as indicated here. That these calculations have some merit is suggested by such facts as that finite-dimensional inertial manifolds are known to exist for certain p.d.e.'s (e.g. [5]).

We consider a nonlinear p.d.e. in one space dimension x , $-\infty < x < \infty$, for a function $A(x, t)$ satisfying

$$A_t = N[\partial_x](A; \mu), \tag{3.1}$$

where N is a nonlinear autonomous differential operator. In applications, N is typically translation invariant, and this leads to an important symmetry in the analysis. As a prototype, we shall think of the complex Ginzburg-Landau equation

$$A_t = \alpha A + \beta |A|^2 A + \gamma A_{xx}, \tag{3.2}$$

applied on the infinite real line. In general, we assume

$$N(0, \mu) = 0, \tag{3.3}$$

i.e., $A = 0$ is a fixed point, and we suppose that when $\mu = 0$, there exists a homoclinic orbit

$$\Gamma: A = A^*(x, t), \quad A^* \rightarrow 0 \text{ uniformly as } t \rightarrow \pm\infty. \tag{3.4}$$

Thus, solitons are not homoclinic orbits, at least not here.

The linearization of N at the origin has solutions $\exp(ikx + \sigma t)$, where σ satisfies a dispersion relation

$$\sigma = \sigma(k); \tag{3.5}$$

for example, that for (3.2) is $\sigma = \alpha - \gamma k^2$. Generally, $\text{Re } \sigma > 0$ for some values of k , $\text{Re } \sigma < 0$ for the rest. We assume that this is the case for (3.5), and denote by U and S those subsets of \mathbb{R} for which $\text{Re } \sigma > 0$ and $\text{Re } \sigma < 0$, respectively. Thus there are functions α^* and β^* such that

$$A^* \sim \int_{-\infty}^{\infty} \alpha^*(k) \exp[ikx + \sigma(k)t] dk \quad \text{as } t \rightarrow -\infty, \tag{3.6}$$

$$A^* \sim \int_{-\infty}^{\infty} \beta^*(k) \exp[ikx + \sigma(k)t] dk \quad \text{as } t \rightarrow +\infty,$$

where $\alpha^* = 0$ for $k \in S$, $\beta^* = 0$ for $k \in U$. We may choose the phase of A^* such that α^* , $\beta^* = O(1)$, and so that $|A^*|$ is maximal at $x = 0$. Our aim, as before, is to map some appropriately defined Σ to itself as illustrated in Figure 1. With a continuous spectrum, the decay of A^* towards 0 is algebraic; but we can still define the equivalent of (2.5), which would be

$$\begin{aligned} \Sigma: |\mathcal{F}[A; k_0]| &= \nu, \\ \Sigma': |\mathcal{F}[A; k_0]| &\sim \nu, \end{aligned} \tag{3.7}$$

where \mathcal{F} is the Fourier transform and we suppose k_0 is the (or a) value where $\text{Re } \sigma = 0$. Suppose A^* intersects Σ and Σ' when $t = t_S$ and $-t_U$, respectively, and $t_S, t_U \gg 1$.

As for the finite-dimensional case, we define α and β when A is on Σ or Σ' by

$$\begin{aligned} A &= \int \alpha(k) \exp[ikx - \sigma(k)t_U] dk \quad \text{on } \Sigma', \\ A &= \int \beta(k) \exp[ikx + \sigma(k)t_S] dk \quad \text{on } \Sigma. \end{aligned} \tag{3.8}$$

Within the box B (bounded by Σ and Σ'), A satisfies

$$A_t = \mathcal{L}[0]A + g(A), \quad (3.9)$$

where

$$g(A) = N(A) - \mathcal{L}[0]A, \quad (3.10)$$

and $\mathcal{L}[0]$ is the derivative of N at $A=0$. If we neglect the quadratic term $g(A)$, then the approximate solution of (3.9) satisfying (3.8) determines α as

$$\alpha(k) = \beta(k)^{\sigma(k)P}, \quad (3.11)$$

where

$$P = \bar{t} + t_S + t_U, \quad (3.12)$$

and \bar{t} is the time of transit from Σ to Σ' .

To map the flow from Σ' back to Σ , we write

$$A = A^*(x, t) + v, \quad (3.13)$$

so that v satisfies

$$v_t = \mathcal{L}[A^*]v + h[A^*, v], \quad (3.14)$$

where

$$h[A^*, v] = N[A^* + v; \mu] - N[A^*, 0] - \mathcal{L}[A^*]v, \quad (3.15)$$

and \mathcal{L} is the Frechet derivative of N at A^* and $\mu=0$. A formal solution to (3.14) can be found using the idea of a Green's operator for the homogeneous equation

$$v_t = \mathcal{L}[A^*]v. \quad (3.16)$$

Specifically, \mathcal{L} generates a fundamental solution $T(t, \tau)$, which is an operator satisfying

$$\frac{\partial T}{\partial t} = \mathcal{L}T, \quad t > \tau, \quad (3.17)$$

$$T(\tau, \tau) = I,$$

in terms of which the solution of (3.16) is

$$v = T(t, t_0)v_0, \quad (3.18)$$

where $v = v_0$ at $t = t_0$. The solution of the inhomogeneous equation (3.14) is then, with $v = v(x, t_0)$ at $t = t_0$,

$$v = T(t, t_0)[v(x, t_0)] + \int_{t_0}^t T(t; \tau)[h(x, \tau)] d\tau. \quad (3.19)$$

The flow at the origin, T_0 , satisfies $\partial T_0 / \partial t = \mathcal{L}[0]T_0$, and is defined by

$$(T_0 u)(x, t) = \int_{-\infty}^{\infty} K_0(x, s, t, \tau)u(s) ds, \quad (3.20)$$

$$K_0(x, s, t, \tau) = \frac{1}{2\pi} \int_{-\infty}^{\infty} \exp[ik(x-s) + \sigma(k)(t-\tau)] dk,$$

and we expect T to be close to T_0 in some sense as $t \rightarrow \pm\infty$.

In a similar way, we can define the Green's function K for (3.16) via

$$\frac{\partial K}{\partial t} = \mathcal{L}[A^*]K, \quad K = K(x, s, t, \tau), \quad (3.21)$$

$$K(x, s, \tau, \tau) = \delta(x-s),$$

whence the semiflow is defined by

$$[T(t, t_0)v](x) = \int_{-\infty}^{\infty} K(x, s, t, t_0)v(s, t_0) ds. \quad (3.22)$$

To derive an expression for T , we note that, if $K \in L_2(\mathbb{R}^2)$, then T is compact, for each fixed t . The spectral representation theorem for compact operators can be stated as follows: if $\psi(x, k; t, \tau)$ is a family of orthonormal eigenfunctions of T^*T satisfying

$$\int_{-\infty}^{\infty} \psi(x, k)\bar{\psi}(x, l) dx = \delta(k-l), \quad (3.23)$$

where T^* is the adjoint of T , then T can be represented as (3.22), where

$$K(x, s, t, \tau) = \int_{-\infty}^{\infty} \Lambda(k; t, \tau)\varphi(x, k; t, \tau)\bar{\psi}(s, k; t, \tau) dk, \quad (3.24)$$

where $|\Lambda|^2$ are eigenvalues of T^*T , and

$$\begin{aligned} T\psi &= \Lambda\varphi, \\ T^*\varphi &= \bar{\Lambda}\psi. \end{aligned} \quad (3.25)$$

In the self-adjoint case, $\varphi = \psi$ and Λ is an eigenvalue of T .

Our natural choice for the functions ψ is to use the Jost solutions [4] satisfying

$$\psi \sim e^{ikx} \quad \text{as } x \rightarrow -\infty. \quad (3.26)$$

If we assume A^* is "localized," i.e. $A^* \rightarrow 0$ as $x \rightarrow \pm\infty$ uniformly, then the asymptotic behavior of (3.5) implies that we can take

$$\Lambda = e^{\sigma(k)x(t-\tau)}, \quad \varphi \sim e^{ikx} \quad \text{as } x \rightarrow -\infty. \quad (3.27)$$

We now wish to construct a result analogous to (2.16) and (2.17). This is rather more subtle than for the ordinary differential equation, since we need the notion of an inverse for T , which may not exist on the whole function space if (e.g.) N is parabolic, i.e., T is a semiflow. We define α^*, β^* by

$$A^* = \int_{-\infty}^{\infty} \alpha^*(k) \exp[ikx - \sigma(k;0)t_U] dk \quad (3.28)$$

on Σ' and

$$A^* = \int_{-\infty}^{\infty} \beta^*(k) \exp[ikx + \sigma(k;0)t_S] dk \quad (3.29)$$

on Σ . The translation invariance of the flow means that for A to be close to a homoclinic orbit, $\alpha \approx \alpha^* e^{-ikQ}$ for some Q , which represents the location (near $x=Q$) of the disturbance (i.e. $A \sim 1$ for x near Q , when A passes from Σ' to Σ). Writing

$$\hat{\alpha} = \alpha - \alpha^* e^{-ikQ}, \quad \hat{\beta} = \beta - \beta^* e^{-ikQ}, \quad (3.30)$$

then v in (3.22) is given by

$$v = \int_{-\infty}^{\infty} \hat{\alpha}(k) \exp[ikx - \sigma(k)t_U] dk \quad \text{on } \Sigma', \quad (3.31)$$

$$v = \int_{-\infty}^{\infty} \hat{\beta}(k) \exp[ikx + \sigma(k)t_S] dk \quad \text{on } \Sigma,$$

and putting $t = -t_U$ on Σ' , $t \approx t_S$ on Σ , (3.19) can be written, using (3.22), as

$$\int_{-\infty}^{\infty} \hat{\beta}(k) e^{ikx + \sigma(k)t_S} dk = \int_{-\infty}^{\infty} K(x, s, t_S, -t_U) \int_{-\infty}^{\infty} \hat{\alpha}(l) e^{ils - \sigma(l)t} dl ds + \int_{-t_U}^{t_S} \int_{-\infty}^{\infty} K(x, s, t_S, \tau) h(s, \tau) ds d\tau. \quad (3.32)$$

We define v at $t=0$ from (3.31), and (3.22):

$$v(x) = \int_{-\infty}^{\infty} K(x, s, 0, -t_U) \int_{-\infty}^{\infty} \hat{\alpha}(l) e^{ils - \sigma(l)t_U} dl ds. \quad (3.33)$$

Now the group property of T implies that

$$\int_{-\infty}^{\infty} K(x, u, t, \tau) K(u, s, \tau, t_0) du = K(x, s, t, t_0) \quad (3.34)$$

if $t_0 < \tau < t$. We formally extend the definition of K for $t < \tau$ by choosing, consistent with (3.34),

$$\int_{-\infty}^{\infty} K(x, u, t_0, t) K(u, s, t, t_0) du = \delta(x - s). \quad (3.35)$$

This is tantamount to defining T^{-1} , and can only be done on a restricted domain; for example we may take the domain of T^{-1} to be $C_0^\infty(\mathbb{R})$.

Using (3.35), Equation (3.33) is

$$\int_{-\infty}^{\infty} \hat{\alpha}(l) e^{ils - \sigma(l)t_U} dl = \int_{-\infty}^{\infty} K(x, u, -t_U, 0) v(u) du. \quad (3.36)$$

Similarly, using (3.34) with $t = t_S$, $t_0 = -t_U$, $\tau = 0$, (3.32) becomes, using the definition of v in (3.33),

$$\int_{-\infty}^{\infty} \hat{\beta}(k) e^{ikx + \sigma(k)t_S} dk = \int_{-\infty}^{\infty} K(x, u, t_S, 0) v(u) du + \int_{-t_U}^{t_S} \int_{-\infty}^{\infty} K(x, s, t_S, \tau) h(s, \tau) ds d\tau. \quad (3.37)$$

We are now in position to make an Ansatz equivalent to (2.16). We suppose $\bar{\psi}(s, k; t, 0) \rightarrow \bar{\psi}_\pm(s, k)$ as $t \rightarrow \pm\infty$ [provided (3.24) can be used for $t < \tau$]. From (3.27), it follows that we may write

$$K(x, s, t, 0) \approx \int_{-\infty}^{\infty} e^{\sigma(k)t} e^{ikx} \bar{\psi}_\pm(s, k) dk \quad (3.38)$$

as $t \rightarrow \pm\infty$, since K approximately satisfies $\partial K / \partial t = \mathcal{L}[0]K$ as $t \rightarrow \pm\infty$. Using (3.38), (3.36) gives

$$\hat{\alpha}(k) \approx \int_{-\infty}^{\infty} \bar{\psi}_-(s, k) v(s) ds, \quad (3.39)$$

which, by (3.23) [in the form $\int_{-\infty}^{\infty} \psi(x, k) \bar{\psi}(s, k) dk = \delta(x - s)$], we may invert as

$$v(x) = \int_{-\infty}^{\infty} \psi_{-}(x, k) \hat{\alpha}(k) dk. \tag{3.40}$$

Inverting (3.37), using (3.38) and (3.40), now yields

$$\hat{\beta}(k) \approx \int_{-\infty}^{\infty} m(k, l) \hat{\alpha}(l) dl + I', \tag{3.41}$$

where

$$m(k, l) = \int_{-\infty}^{\infty} \bar{\psi}_{+}(s, k) \psi_{-}(s, l) ds \tag{3.42}$$

and

$$I' = \int_{-t_U}^{t_S} \int_{-\infty}^{\infty} \int_{-\infty}^{\infty} \bar{\psi}_{+}(u, k) K(u, s, 0, \tau) h(s, \tau) du ds d\tau. \tag{3.43}$$

Formally, our method only shows that the operator M' taking $\hat{\alpha}$ to $\hat{\beta}$ defined on the Hilbert space $L_2(\mathbb{R})$, coincides with that defined by (3.41) on the subspace such that v in (3.40) is in $C_0^{\infty}(\mathbb{R})$. However, (3.41) is densely defined and compact, and since M' is also compact, (3.41) trivially extends to the whole space. Since $h = O(\mu)$, then also $I' \sim \mu$.

A one-dimensional map

Approximately, we have

$$\begin{aligned} \alpha(k) &= \beta(k) e^{\sigma(k)P}, \\ \beta' - \beta^* e^{-ikQ} &= \int_I m(k, l) \{ \alpha(l) - a^*(l) e^{ilQ} \} dl + \mu c e^{-ikQ}, \end{aligned} \tag{3.44}$$

where c is independent of Q in view of (3.30), and because (as one can show) $I' e^{ikQ}$ is also. [This is most easily seen by looking at (3.37) and realizing $K = K(x - Q, s - Q, t_S, \tau)$, $h = h(s - Q)$.] Furthermore, the eigenfunctions ψ of T^*T depend on Q as

$$\psi(x, k; Q) = e^{ikQ} \psi_0(x - Q, k), \tag{3.45}$$

since $\mathcal{L} = \mathcal{L}[A^*(x - Q, t)]$, and taking account of (3.26). Therefore, (3.42) implies

$$m(k, l) = M(k, l) e^{i(l-k)Q}, \tag{3.46}$$

where

$$M(k, l) = \int_{-\infty}^{\infty} \bar{\psi}_{0+}(s, k) \psi_{0-}(s, l) ds. \tag{3.47}$$

We put

$$\begin{aligned} \alpha e^{ikQ} &= A, & \beta e^{ikQ} &= B, \\ A_U &= \alpha_U^* + a_U, & B_S &= \beta_S^* + b_S, \end{aligned} \tag{3.48}$$

so that

$$\begin{aligned} B_U &= e^{-\sigma_U(k)P} (\alpha_U^* + a_U), \\ A_S &= e^{\sigma_S(k)P} (\beta_S^* + b_S), \\ B_S^{\dagger} &= \int_U M_S(k, l) a_U(l) dl + \int_S M_S(k, l) A_S(l) dl + \mu c_S, \\ B_U^{\dagger} &= \int_U M_U(k, l) a_U(l) dl + \int_S M_U(k, l) A_S(l) dl + \mu c_U, \end{aligned} \tag{3.49}$$

where $M_U = M$ with $k \in U$, $M_S = M$ with $k \in S$, and U is $\{k \in \mathbb{R} | \text{Re } \sigma(k) > 0\}$, $S = \{k \in \mathbb{R} | \text{Re } \sigma(k) < 0\}$.

We restrict attention to neighborhoods of the sets

$$\begin{aligned} \Lambda_0: \beta_U &= e^{-\sigma_U(k)P - ikQ} \alpha_U^* & \text{in } \Sigma, \\ \Lambda'_0: \alpha_S &= e^{\sigma_S(k)P - ikQ} \beta_S^* & \text{in } \Sigma', \end{aligned} \tag{3.50}$$

and anticipate defining β'_U in a similar way.

We omit any attempt to discuss the geometric structure of the invariant set, and concentrate on the approximate form of (3.49)_U, which is this:

$$\begin{aligned} \mathcal{M}_{UU} a_U &\stackrel{\text{def}}{=} \int_U M_U(k, l) a_U(l) dl \\ &\approx \beta'_U e^{ikQ} - \left\{ \int_S M_U(k, l) e^{\sigma_S(l)P} \beta_S^* dl + \mu c_U \right\}. \end{aligned} \tag{3.51}$$

Now notice that $u = \partial A^* / \partial t$ and $v = \partial A^* / \partial x$ both satisfy the equation $u_t = \mathcal{L}[A^*]u$, and $u \sim \int \sigma(k) \alpha^*(k) e^{ikx + \sigma(k)t} dk$ as $t \rightarrow -\infty$, $u \sim \int \sigma(k) \beta^*(k) e^{ikx + \sigma(k)t} dk$ as $t \rightarrow +\infty$ (here $Q = 0$): similarly for v , with σ replaced by ik .

It follows from (3.44) that (approximately)

$$\sigma(k)\beta^*(k) = \int_I M(k,l)\sigma(l)\alpha^*(l) dl, \tag{3.52}$$

$$ik\beta^*(k) = \int_I M(k,l)il\alpha^*(l) dl,$$

and since $\beta_U^* = 0 = \alpha_S^*$, we have

$$\int_U M_U(k,l)\sigma(l)\alpha^*(l) dl = 0, \tag{3.53}$$

$$\int_U M_U(k,l)l\alpha^*(l) dl = 0.$$

The null space of \mathcal{A}_{UU} is thus of dimension two. Suppose η_1, η_2 span the null space of the adjoint operator \mathcal{A}_{UU}^* (which is of dimension two by the Fredholm alternative). Then (3.51) can only be inverted if its right-hand side is orthogonal to η_j ; that is,

$$\begin{aligned} & \int_U \beta_U^*(k) e^{ikQ} \bar{\eta}_j(k) dk \\ &= \int_{k \in U} \int_{l \in S} M_U(k,l) e^{\sigma_S(l)P} \beta_S^*(l) \bar{\eta}_j(k) dl dk + \mu \int_U c_U(k) \bar{\eta}_j(k) dk \end{aligned} \tag{3.54}$$

for $j = 1, 2$.

Consider first the case where there is a single translation-invariant family of homoclinic orbits. Following (3.49) and (3.50), we define

$$\beta_U^* = e^{-\sigma_U(k)P' - ikQ'} (\alpha_U^* + a_U^*), \tag{3.55}$$

whence (3.54) is, approximately,

$$\int_U \exp[-\sigma_U(k)P' - ik(Q' - Q)] w_j(k) dk = \int_S \exp[\sigma_S(l)P] y_j(l) dl + \mu, \tag{3.56}$$

where

$$w_j(k) = \frac{\alpha_U^*(k) \bar{\eta}_j(k)}{\int_U c_U(k) \bar{\eta}_j(k) dk}, \tag{3.57}$$

$$y_j(l) = \frac{\beta_S^*(l) \int_U M_U(k,l) \bar{\eta}_j(k) dk}{\int_U c_U(k) \bar{\eta}_j(k) dk}$$

[notice that $y_j \neq 0$, since, although $\int_U \bar{M}_U(k,l) \eta_j(k) dk = 0$ for $l \in U$, this is not so for $l \in S$, where y_j is defined].

The method of steepest descents approximates integrals such as those in (3.56) for large P and P' by deforming the contours in the complex k (or l) plane so that $\text{Im } \sigma$ (for \int_S) or $\text{Im}[\sigma + ik(Q' - Q)/P']$ (for \int_U) is constant along the deformed contours. Thus the deformed contours consist of pieces going through points $k = k_m$ where $\text{Re } \sigma = 0$, supplemented if necessary by appropriate saddle-point contours. As an illustration, the dispersion relation from (3.2),

$$\sigma = \alpha - \gamma k^2, \quad \alpha \in \mathbb{R}, \quad \gamma \in \mathbb{C}, \tag{3.58}$$

induces the deformations shown in Figure 3 (for $\text{Re } \gamma > 0, \text{Im } \gamma < 0$). At B and E we have $k = -k_0$ and k_0 , where $k_0 = (\alpha/\gamma_R)^{1/2}$, $\text{Re } \sigma = 0$, and ABC and FED are defined by

$$\sigma(k) = \sigma(k_m) - s, \quad s \in \mathbb{R}. \tag{3.59}$$

The appropriate deformation of $S = (-\infty, -k_0) \cup (k_0, \infty)$ is to $AB \cup ED$, whereas $U = (-k_0, k_0)$ must be deformed to $BC \cup COF \cup FE$, where the saddle-point contour through 0 for the integral over U is defined by

$$\sigma(k) + ik\Omega = \sigma(0) - t^2, \quad t \in \mathbb{R}, \tag{3.60}$$

where

$$\Omega = \frac{Q' - Q}{P'}. \tag{3.61}$$

is assumed $O(1)$. In general, any necessary saddle-point contours will not contribute, unless $\text{Re } \sigma = 0$ there (an example is the Kuramoto-Sivaskinsky equation [14]).

At leading order, the application of Laplace's method to the integrals over the deformed contours gives

$$\int_S e^{\sigma_S(l)P} y_j(l) dl \sim \sum_m \mp \frac{y_j(k_m)}{\sigma'(k_m)} \frac{e^{i\omega_m P}}{P}, \tag{3.62}$$

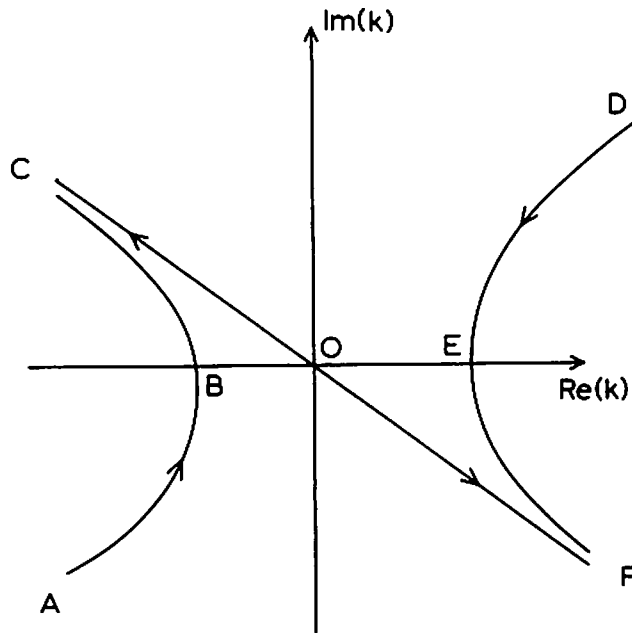


Figure 3. Steepest-descent contours for the dispersion relation (3.58). The arrows indicate the direction of increasing $\text{Re } \sigma$ (here $\gamma_R > 0, \gamma_I < 0$).

where $\text{Re } \sigma(k_m) = 0, \text{Im } \sigma(k_m) = \omega_m$, and the upper sign is taken if the deformed contour is directed away from k_m . Similarly, we find, with $Q' - Q \sim P'$,

$$\int_U e^{-\sigma_U(k)P' - ik(Q' - Q)} w_j(k) dk \sim \sum_m \pm \frac{w_j(k_m) e^{-i\omega_m P' - ik_m L}}{\sigma'(k_m) P' - iL}, \quad (3.63)$$

where

$$L = Q' - Q. \quad (3.64)$$

If $\text{Re } \sigma = 0$ at $k = k_m, m = 1, 2, \dots$, then the form of the map is

$$\sum_m \frac{c_{jm} e^{-i\omega_m P' - ik_m L}}{P' + i\lambda_m L} = \sum_m \frac{d_{jm} e^{i\omega_m P}}{P} + \mu, \quad (3.65)$$

with $j = 1, 2$ (assuming saddle points do not contribute). If we suppose the system $A_j = N(A)$ is real, then k_m occur in pairs $\pm k_m$ with frequency $\pm \omega_m$ and coefficients $\pm \lambda_m$, and c_{jm} occur in complex conjugate pairs. For $j = 1, 2$, (3.65) therefore provides two real equations for the two real unknowns P' and L .

The simplest case is where $N(A)$ is a real, symmetric, scalar operator, so that σ is real, $\lambda_m = \pm \lambda$ is real, and $\omega_m = 0$. Then (3.65) can be written

$$\begin{aligned} c_1 \zeta + \bar{c}_1 \bar{\zeta} &= \mu + \frac{d_1}{P}, \\ c_2 \zeta + \bar{c}_2 \bar{\zeta} &= \mu + \frac{d_2}{P}, \end{aligned} \quad (3.66)$$

where $d_i \in \mathbb{R}$, and

$$\zeta = \frac{e^{-ik_0 L}}{P' + i\lambda L}. \quad (3.67)$$

Solving for ζ , we get

$$\frac{e^{-ik_0 L}}{P' + i\lambda L} = \frac{A}{P} + \mu B, \quad (3.68)$$

where A and B are generally complex. Periodic orbits in the flow correspond to fixed points $P = P'$ with $L = 0$, and in general these do not exist. Multiple fixed points with $P = P', L \neq 0$ do exist, and satisfy $\mu \sim P^{-1}$ as $P \rightarrow \infty$. If, for example, A and B are real, then we have

$$L \sim n\pi/k_0, \quad n \in \mathbb{Z}, \quad \mu \sim P^{-1} \quad (3.69)$$

as $P \rightarrow \infty$; see Figure 4. There are countably many of these solutions which have the form of traveling modulated solitary waves. The period of modulation is

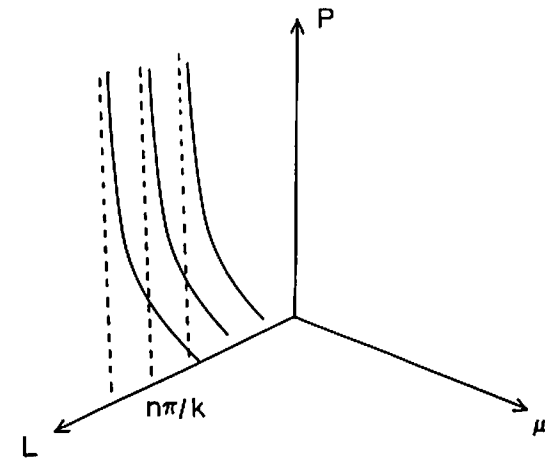
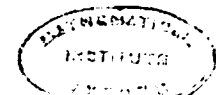


Figure 4. Bifurcation diagram for a symmetric, real, scalar equation, with $k_m = \pm k_0$. A countable family of modulated traveling-wave solutions is generated.



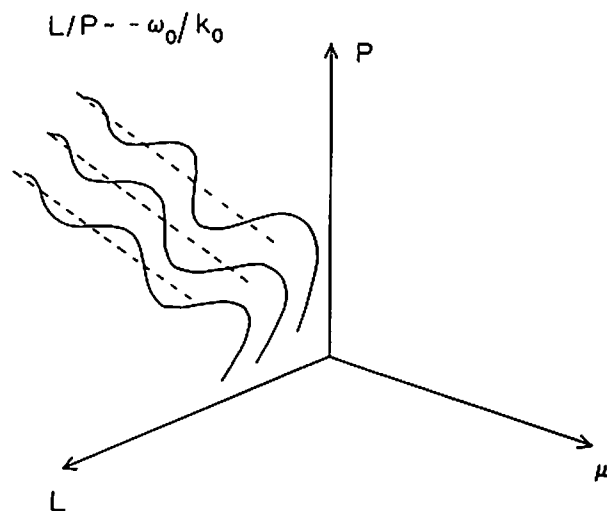


Figure 5. Bifurcation diagram for an asymmetric, real, scalar equation, with $k_m = \pm k_0$. A countable family of doubly periodic, modulated traveling-wave solutions is produced, all with the same wave speed, $\sim -\omega_0/k_0$.

$P \sim \mu^{-1}$, and the wave speed is $L/P \sim n\pi/\mu k_0$.

If $N(A)$ is real but not symmetric, then $\omega_m \neq 0$. If $k_m = \pm k_0$ as before, then $\lambda_m = \pm \lambda$ (but complex), and the equivalent of (3.68) is

$$\frac{e^{-i\omega_0 P' - ik_0 L}}{P' + i\lambda L} = \mu B + \frac{A}{P} \cos(\omega P + \theta). \quad (3.70)$$

Fixed points $P = P'$, $L = \text{constant}$ exist, for which we find $L, P \rightarrow \infty$ together and

$$\begin{aligned} \mu &\sim \frac{1}{P} \cos(\omega_0 P + \bar{\theta}), \\ \omega_0 P + k_0 L &\sim n\pi, \quad n \in \mathbb{Z}. \end{aligned} \quad (3.71)$$

This is analogous to Shil'nikov's results for ordinary differential equations [10]. These are countably many of these orbits, which represent modulated, doubly periodic traveling waves with periods $2\pi/\omega_0$ and P , and the wave speed is the marginal phase speed $L/P \sim -\omega_0/k_0$; see Figure 5.

4. Discussion

The development here is purely theoretical, but there is some indication from numerical work that the ideas may be fruitful. Bretherton and Spiegel [3]

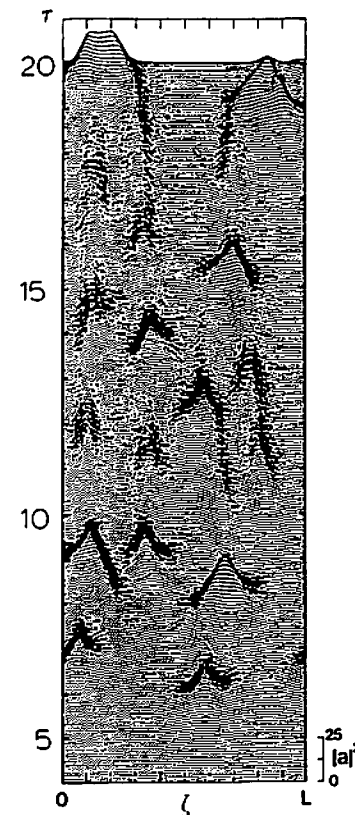


Figure 6. A numerical integration of the Ginzburg-Landau equation $a_t = \alpha a + \beta |a|^2 a + \gamma a_{\zeta\zeta}$ ($\alpha = 1$, $\beta = i$, $\gamma = 1 + i$), with periodic conditions on the domain $0 < \zeta < L = 20$. This figure is reproduced from [3] with permission. The isolated "bursts" resemble the kind of homoclinic pulses which are analysed here.

integrated the Ginzburg-Landau equation numerically, and discovered solutions which behaved aperiodically in space and time (see Figure 6); this solution is very suggestive of the generative process in Section 3). At other parameter values, they found the generation of a "sea of solitons." Keefe [15], on a finite domain, found evidence of nearly homoclinic quasiperiodic solutions in the Ginzburg-Landau equation. Hyman et al. (1986) reported similar solutions (modulated traveling waves), as well as numerous homoclinic structures, for the Kuramoto-Sivashinsky equations.

Whereas modulated wave structures are consistent with homoclinic bifurcations for partial differential equations on an infinite domain, they are not consistent with finite-dimensional truncations which should be accurate on a

finite domain [5]. The obvious question is how periodic and quasiperiodic orbits are lost as the domain size l is increased: i.e., how large does l have to be to be "nearly infinite"? Since P and L in (3.65) are $O(\mu^{-1})$, it is an obvious conjecture that the infinite-domain analysis will apply if $l > \mu^{-1}$; hence, we may expect a complicated transition to occur when $l \sim \mu^{-1}$, and we might conjecture that this provides a convenient dividing region between "chaotic" and more complicated spatiotemporally chaotic dynamics.

The effect of an infinite (and autonomous) x domain is to generate an effectively two-dimensional map for P (time between pulses) and Q (space between pulses). It is an obvious extension to suppose that if there are two infinite space domains (e.g. convection in a large box), then we shall obtain a three-dimensional map for (P, Q, R) . We would thus expect skewed modulated traveling waves.

In terms of applicability, we have in view thermal convection as a system which can be brought to a "turbulent" state within an essentially bounded framework. The breakdown of regular flow as the Rayleigh number increases, and the occurrence of sporadic thermals at random locations, suggests that these may be interpreted as heteroclinic loops between quasistationary convectionless states. In that case, the ideas here may be brought to bear.

The other main application we have in view is that of transition in shear flow. The bifurcation analysis presented here bears some resemblance to a simple type of turbulent burst [29], and the fact that the evolution of a transverse line vortex in a shear flow can be modeled by a perturbation of the nonlinear Schrödinger equation [11, 1] is highly suggestive in this context (as well as the fact that Aref and Flinchem's numerical results [1] are also suggestive of the "bursting" process revealed in Section 3).

Acknowledgments

This research was supported in part by a grant from the Research Corporation. Many thanks for their help to Andy Bernoff, Paul Glendinning, and Jeff DeWynne.

References

1. H. AREF and E. P. FLINCHEM, Dynamics of a vortex filament in a shear flow, *J. Fluid Mech.* 148:477-497 (1984).
2. A. ARNEODO, P. COULLET, and C. TRESSER, Oscillations with chaotic behavior: An illustration of a theorem by Shil'nikov, *J. Statist. Phys.* 27:171-182 (1982).
3. C. S. BRETHERTON and E. A. SPIEGEL, Intermittency through modulational instability, *Phys. Lett.* 96A:152-156 (1983).
4. R. K. DODD, J. C. EILBECK, J. D. GIBBON, and H. C. MORRIS, *Solitons and Nonlinear Wave Equations*, Academic, London, 1982.
5. C. R. DOERING, J. D. GIBBON, D. D. HOLM, and B. NICOLAENKO, Low-dimensional behavior in the complex Ginzburg-Landau equation, *Nonlinearity* 1:279-309 (1988).
6. J. P. ECKMANN, Roads to turbulence in dissipative dynamical systems, *Rev. Mod. Phys.* 53:641-652 (1981).
7. P. R. FENSTERMACHER, H. L. SWINNEY, and J. P. GOLLUB, Dynamical instabilities and the transition to chaotic Taylor vortex flow, *J. Fluid Mech.* 94:103-129 (1979).
8. A. C. FOWLER, Homoclinic bifurcations in n dimensions, *Stud. Appl. Math.* 83:193-209 (1990).
9. P. GASPARD, R. KAPRAL, and G. NICOLIS, Bifurcation phenomena near homoclinic systems: A two-parameter analysis, *J. Statist. Phys.* 35:697-727 (1984).
10. P. GLENDINNING and C. SPARROW, Local and global behaviour near homoclinic orbits, *J. Statist. Phys.* 35:645-696 (1984).
11. H. HASIMOTO, A soliton on a vortex filament, *J. Fluid Mech.* 51:477-485 (1972).
12. TH. HERBERT, Modes of secondary instability in plane Poiseuille flow, in *Turbulence and Chaotic Phenomena in Fluids* (T. Tatsumi, Ed.), North-Holland, Amsterdam, 1984, pp. 53-58.
13. L. N. HOWARD, Convection at high Rayleigh number, in *Proceedings of the Eleventh International Congress of Applied Mechanics* (H. Görtler, Ed.), 1966, pp. 1109-1115.
14. J. M. HYMAN, B. NICOLAENKO, and S. ZALESKI, Order and complexity in the Kuramoto-Sivashinsky model of weakly turbulent interfaces, *Phys. D* 23, 265-292 (1986).
15. L. R. KEEFE, Dynamics of perturbed wavetrain solutions to the Ginzburg-Landau equation, *Stud. Appl. Math.* 73:91-153 (1985).
16. A. LIRCHBER, C. LAROCHE, and S. FAUVE, Period-doubling cascade in mercury, a quantitative measurement, *J. Phys. Lett.* 43:L211-L216 (1982).
17. E. N. LORENZ, Deterministic non-periodic flow, *J. Atmospheric Sci.* 20:131-141 (1963).
18. S. A. MASLOWE, Shear flow instabilities and transition, in *Hydrodynamic Instabilities and the Transition to Turbulence* (H. L. Swinney and J. P. Gollub, Eds.), 2nd ed., Springer-Verlag, Berlin, 1985, pp. 181-228.
19. S. ORSZAG and A. T. PATERA, Secondary instability of wall bounded shear flows, *J. Fluid Mech.* 128:347-385 (1983).
20. L. P. SHIL'NIKOV, A case of the existence of a countable number of periodic motions, *Soviet Math. Dokl.* 6:163-166 (1985).
21. L. P. SHIL'NIKOV, The existence of a denumerable set of periodic motions in four-dimensional space in an extended neighbourhood of a saddle-focus, *Soviet Math. Dokl.* 8:54-58 (1967).
22. L. P. SHIL'NIKOV, A contribution to the problem of the structure of an extended neighbourhood of a rough equilibrium state of saddle-focus type, *Mat. Sb.* 10:91-102 (1970).
23. C. T. SPARROW, *The Lorenz Equations: Bifurcations, Chaos, and Strange Attractors*, Springer-Verlag, Berlin, 1982.
24. E. M. SPARROW, R. B. HUSAR, and R. J. GOLDSTEIN, Observations and other characteristics of thermals, *J. Fluid Mech.* 41:793-800 (1970).
25. E. A. SPIEGEL, Chaos, A mixed metaphor for turbulence, *Proc. Roy. Soc. London Ser. A* 413:87-95 (1987).
26. J. T. STUART, On the non-linear mechanics of wave disturbances in stable and unstable parallel flows, *J. Fluid Mech.* 9:353-370 (1960).
27. N. TAMAI, and T. ASAIDA, Sheetlike plumes near a heated bottom plate at large Rayleigh number, *J. Geophys. Res.* 89:727-734 (1984).
28. C. TRESSER, About some theorems by L. P. Shil'nikov, *Ann. Inst. H. Poincaré* 40:441-461 (1984).
29. S. E. WIDNALL, Growth of turbulent spots in plane Poiseuille flow, in *Turbulence and Chaotic Phenomena in Fluids* (T. Tatsumi, Ed.), North-Holland, Amsterdam, pp. 93-98.
30. S. WIGGINS, *Global Bifurcations and Chaos*, Appl. Math. Sci. 73, Springer-Verlag, Berlin, 1988.

OXFORD UNIVERSITY

(Received March 22, 1990)